Application Note

No. 63

Foods

Microscopic Mass Spectrometry Imaging Reveals Specific Distributions of Curcumin Species Inside Dried Turmeric

Shuichi Shimma [*1], Takehito Sagawa [*2]

Foods

■ Abstract

Plants contain a variety of secondary metabolites, many of which are known to be various useful substances, as represented by spices and herbal medicines. To date, however, few reports have examined the 3-dimensional distribution of those substances. In this Application Note, the spatial distribution of curcumin, which is one of the main components of turmeric root, was visualized using a dried turmeric sample. Because dried turmeric samples are extremely hard and sectioning was impossible with a conventional cryomicrotome, we developed a new sectioning method in this research and analyzed the 2-dimensional distributions of sections cut in different directions. The result suggests that curcumin forms tube-shaped compartments in the turmeric root. The distributions of curcumin analogues were also found to be similar to that of curcumin. This new perspective in botany, that is, the specific distributions of secondary metabolites in plants, was revealed by high spatial resolution mass spectrometry imaging (MSI) using the Shimadzu iMScope imaging mass microscope. (Fig. 1 shows the new model, iMScope QT.) In the future, knowledge of the specific distributions of components in plants is expected to contribute to improvement of production processes such as improved extraction methods for active ingredients.

Fig. 1 iMScope QT

*1   Osaka University, Graduate School of Engineering
*2   S&B Foods Inc.

1. Introduction

Although it is possible to visualize the internal structures of plants with a microscope, the technical problem of observing the molecular distribution in plants cannot be answered so simply, as it is impossible to observe the distribution of molecules with a microscope alone. Computed tomography (CT) is one conceivable technique for observing the internal structure. Fig. 2 shows an example of images of turmeric actually captured by X-ray CT. In the image of fresh turmeric in Fig. 2(A), the internal structure appears uniform, but in the image of dried turmeric in Fig. 2(B), a nodular structure can be observed in the interior. If the cross section is examined by actually cutting the sample, it is clear that the internal structure captured by X-ray CT is indeed accurate. However, only structural information can be obtained by this CT technique, and the distribution of components is still unknown.

Fig. 2 Observation of Internal Structure of Turmeric by X-Ray CT
(A) Fresh turmeric   (B) Dried turmeric

Mass spectrometry imaging (MSI) is a technique in which mass spectrometry is conducted by direct ionization of the components in a sample, the analytical data are then developed in 2 dimensions (2D), and information on the distributions of components is obtained based on 2D analytical data from multiple locations. In recent years, MSI has also been used with non-animal samples, and application to various objects has been reported, including plants [1]-[4], insects [5]-[7] and microorganisms [8]-[13]. For example, Taira et al. reported the detailed distribution of ginsenoside in ginseng, and discovered that ginsenoside is concentrated at the tip of the root [14]. Although numerous reports [15]-[21] have noted this kind of accumulation of secondary metabolites in plants, no previous reports have investigated their 3-dimensional distribution. Therefore, in this Application Note, we propose the technique described below for estimation of the 3-dimensional spatial distribution of secondary metabolites by applying MSI to a dried spice (turmeric root) [22]. Raw materials for spices and herbal medicines, as represented by turmeric root, have a variety of shapes like the complex shape of ginger. When verifying the spatial distribution of components in tissue, it is
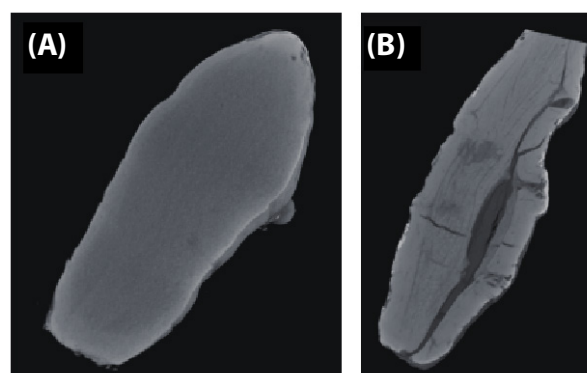
necessary to conduct MSI of sections taken from various angles. In past research, Harada et al. reported that the distribution of 6-gingerol in raw ginger has a granular form [23]. If the distributions of 6-gingerol in a section taken in the longitudinal direction (axial section, Fig. 3(A)) and a section taken in the direction of the short axis (radial section, Fig. 3(B)) of ginger are actually compared, it can be understood that the area values are different, even in the same grain (Fig. 3(C)). This implies that the grains are ellipsoidal, and not perfectly spherical, in shape. In other words, it is possible to understand the 3-dimensional distribution of secondary metabolites in a plant by an analysis of the cross-sectional images captured from different angles.

In this research, we also propose a new sample preparation method for dried spices. Dried spices are targeted in this study, considering the limited availability of fresh raw materials. Although sectioning of samples is essential for MSI, sectioning of dried samples is difficult or impossible owing to their extreme hardness. As a solution to this problem, in this Application Note, we examined two sectioning methods and proposed the optimum technique.
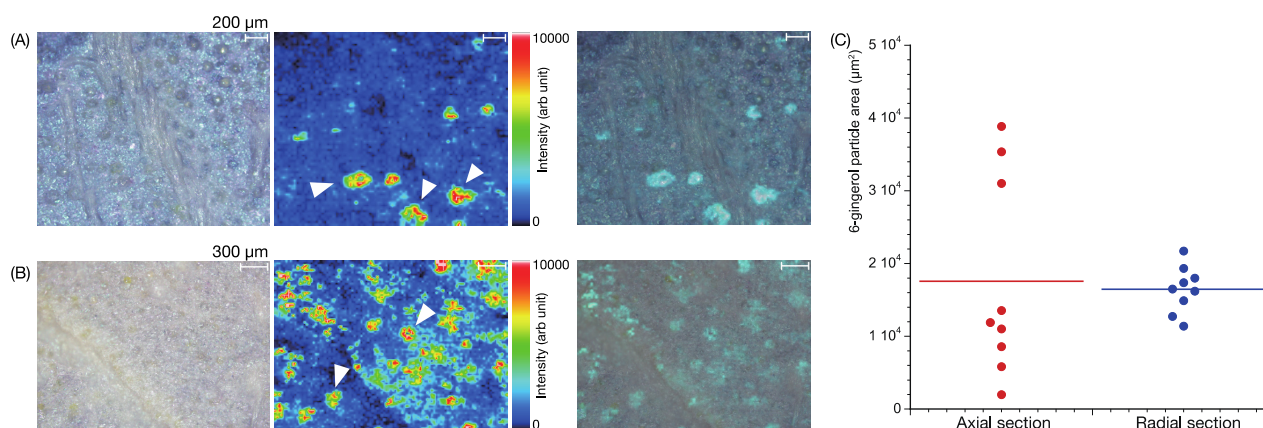

Fig. 3 Distribution of 6-Gingerol in Fresh Ginger
(A) Axial section, (B) Radial section, (C) Plots of area of obtained grain shapes

The axial section contains a wide distribution of grain sizes, from extremely large to small grains, whereas the grains in the radial section have a comparatively uniform area. Arrow-head: Accumulation of 6-gingerol

2. Experiment

2-1. Reagents

9-aminoacridine (9-AA) was purchased from Tokyo Chemical Industry Co., Ltd. (Tokyo). Methanol was purchased from FUJIFILM Wako Pure Chemical Corporation (Osaka). Ultrapure water produced with a GenPure™ UV-TOC xCAD Plus (Thermo Fisher Scientific Inc.) was used.

2-2. Preparation of Sample Sections

Dried turmeric root was provided by S&B Foods Inc. In this Application Note, a dicing machine (YAC DAStech, Inc., Saitama) and a *kanna* (Japanese planer) (Matsusaku-syouten, Shizuoka) were used to section the hard dried turmeric root (Fig. 4(A), (B)). A sample thickness of 500 μm was obtained when using the dicing machine, and a thickness of 75 μm was obtained with the *kanna* (measured using a micrometer). The obtained slices were fixed on ITO slide glass (no MAS coat, surface resistance 100 Ω/m^2, Matsunami Glass Ind., Ltd., Osaka) using conductive double-sided adhesive tape purchased from 3M (United States).

2-3. Matrix Supply

In order to detect curcumin in turmeric, 9-AA was vapor-deposited on the sample surface as the matrix using an iMLayer™ (Shimadzu Corporation), and was then recrystallized [24]-[25]. The thickness of the vapor-deposited matrix was 0.5 μm, and 5 % methanol was used as the solvent for recrystallization.

2-4. Mass Spectrometry Imaging

MSI was conducted using an iMScope (Shimadzu). The laser irradiation count was 100/spot, and measurements were conducted in the negative ion mode. The mass range used in the measurements was *m/z* 250 to 450, and MS/MS of [M-H]$^-$ 367.11 was also carried out for confirmation of curcumin (data not shown). The laser intensity was set to 45, and the detector voltage was 2.1 kV in all measurements.

2-5. Image Reconstruction and Analysis

Image reconstruction was done using Imaging MS Solution™ (Shimadzu), and the analysis of the particle shapes in the obtained images was carried out with Image J and the analytical software R. The obtained distribution images were normalized by TIC (total ion current).
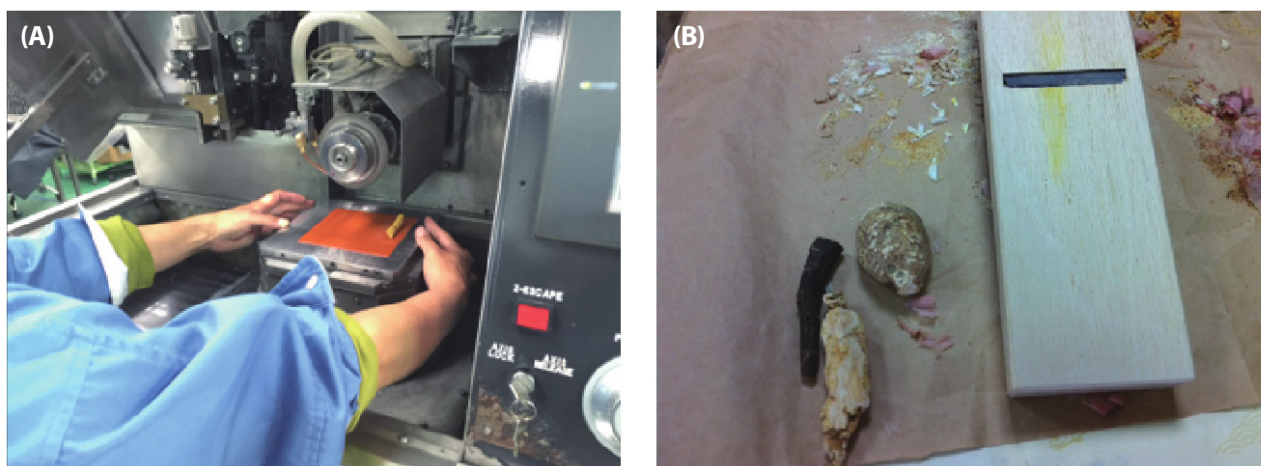

Fig. 4 Dried Turmeric Sectioning Methods Examined in this Research
(A) Dicing machine, (B) *Kanna* (Japanese planer)

3. Results

3-1. Evaluation of Sectioning Method and Evaluation of Curcumin Distribution

To confirm the ionization of curcumin by MALDI, the measured mass spectrum was searched in the database (METLIN https://metlin.scripps.edu/) and it was found that detection by the negative ion mode was considered satisfactory. Accordingly, measurements of curcumin were carried out by negative ion detection mode using 9-AA as the matrix. Two other general matrixes, α-cyano-4-hydroxycinnamic acid (CHCA) and 2,5-dihydroxybenzoic acid (DHB), were also used for confirmation of peak intensity, but a higher peak intensity was obtained when using 9-AA.

Fig. 5 shows the structure of the target compound curcumin, the results of the evaluation of sectioning, and the results of image analysis. Since curcumin has the structure shown in Fig. 5(A), m/z 367.11 is detected as the deprotonated ion in measurements by the negative ion mode using 9-AA. Fig. 5(B) and Fig. 5(C) show a comparison of the distributions of this m/z 367.11 in the axial sections and the radial sections obtained with the dicing machine and the *kanna*. In the axial sections in Fig. 5(B), curcumin is distributed over the entire surface of the sample prepared with the dicing machine, whereas a granular distribution was observed with the *kanna*. In the radial sections in Fig. 5(C), both sections showed a granular distribution. However, in the sections prepared with the dicing machine, the distributions were unclear in both the axial section and the radial section.
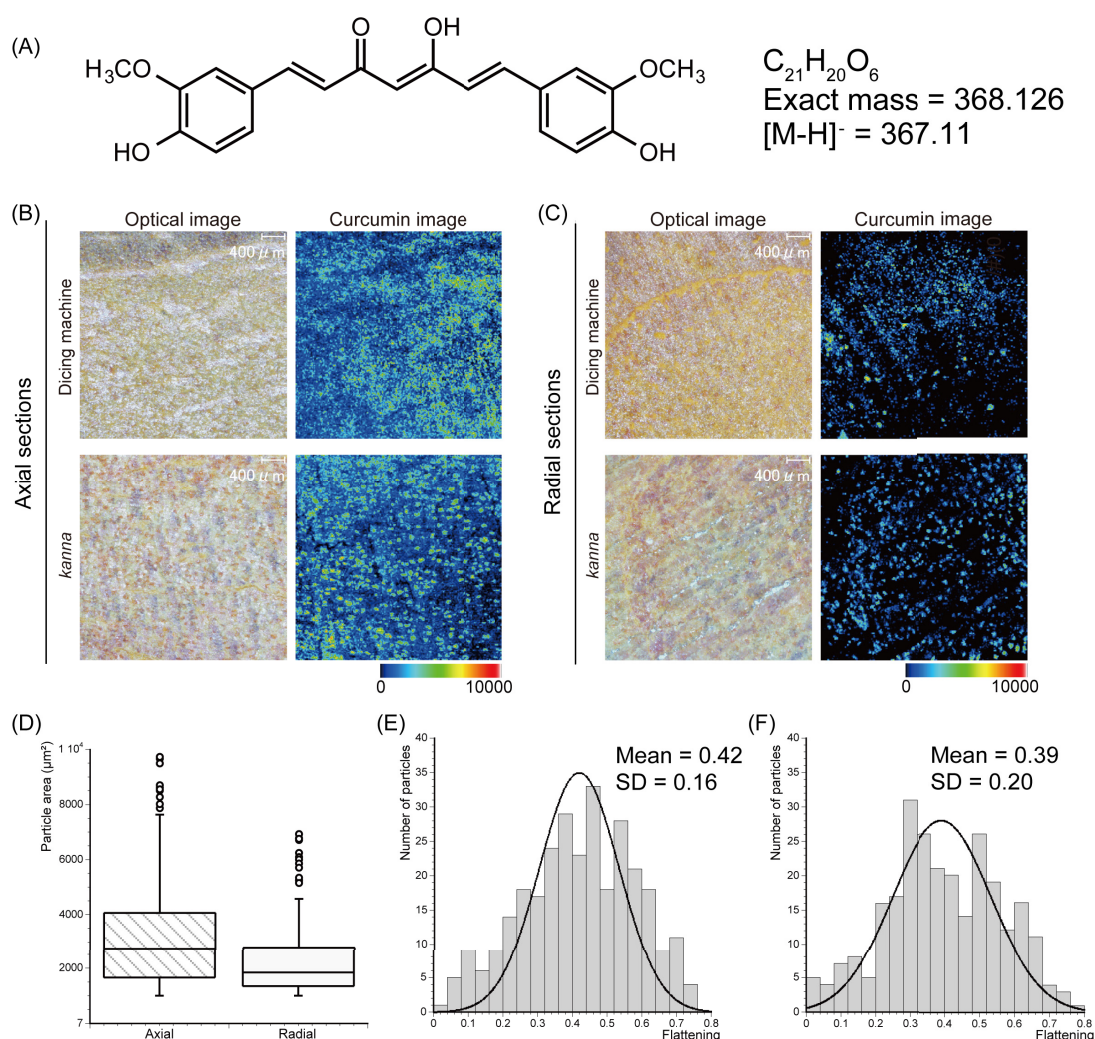

Fig. 5 Chemical Structural Formula of Curcumin, Evaluation of Sectioning with Dicer and *kanna*, and Image Analysis of Particles

(A) Chemical structural formula of curcumin

(B) Comparison of dicing machine and *kanna* in axial section

(C) Comparison of dicing machine and *kanna* in radial section

(D) Comparison of areas of particles obtained by axial and radial sectioning with *kanna*

(E) Oblateness distribution of obtained particles in axial section

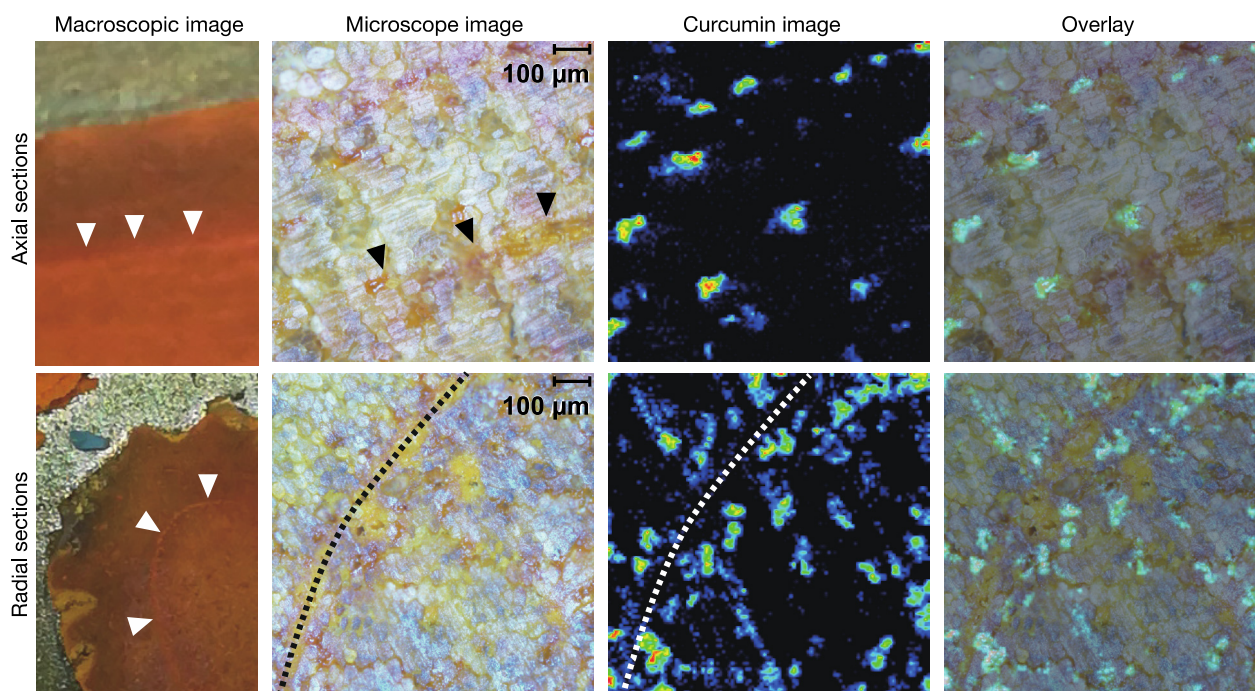(F) Oblateness distribution of obtained particles in radial section

Fig. 6 Distribution of Curcumin at High Resolution
(Upper row): Distribution of curcumin in axial section, (Bottom row): Distribution of curcumin in radial section (pixel size: 5 μm)

The axial section shows a regular arrangement of curcumin particles, but in the radial section, the curcumin particles are distributed along the inner side of a circular ring.

Looking at the distribution results for the axial and radial sections obtained with the *kanna*, the obtained particle shapes are different in the two sections. In order to evaluate the results quantitatively, an image analysis of the particle shape was carried out. In particular, as shown in Fig. 5(D), the particle area tended to be larger in the axial section than in the radial section. In addition, when the oblateness of the particles was calculated from the particle shape, the particles in the axial section had a distribution with an average value of 0.42 (standard deviation: 0.16), while those in the radial section had an average value of 0.39 (standard deviation: 0.20).

3-2. Evaluation of Curcumin Distribution by High Spatial Resolution MSI

The curcumin distribution in microscopic regions of the turmeric was visualized with the iMScope because imaging with resolution of 5 μm can be achieved. Fig. 6 shows the obtained results. The upper row in Fig. 6 shows the results for the axial section with low magnification (wide target) and high magnification (narrow target) images, together with the distribution of curcumin in the high magnification image. The bottom row in Fig. 6 shows the results for the radial section. In the optical images of the axial section, a distinctive structure running in the horizontal direction can be observed, as shown by the arrowheads, and the

curcumin appears to have a regular arrangement independent of that structure.

On the other hands, in the radial section, a similarly distinct but circular structure can also be seen (as shown by the dotted lines). The particle density of the curcumin is extremely high on the inner side of this ring, but not distributed on the ring itself.

3-3. Distinctive Arrangement of Curcumin Particles in Axial Section

It is suggested that the curcumin in the axial section is arranged regularly. To evaluate this point quantitatively, the pixel information for the curcumin distribution in the axial section obtained in Fig. 6 was projected on a coordinate system. Then the positions of the pixels that represent the center of gravity of the particles were calculated, and a linear regression was drawn. Fig. 7 shows the results of this procedure. The coefficient of determination of the linear regression of the center-of-gravity pixels suggests that these particles are arranged on a straight line. Moreover, since the values of the obtained slopes are extremely close, it was also suggested that an extremely regular structure exists in the turmeric tissue. Among the axial sections (sections taken from long axis of the sample), Fig. 8 shows the imaging results obtained in a section near the epidermis. As well as a particle-shaped distribution, a linear distribution can also be observed in this figure.
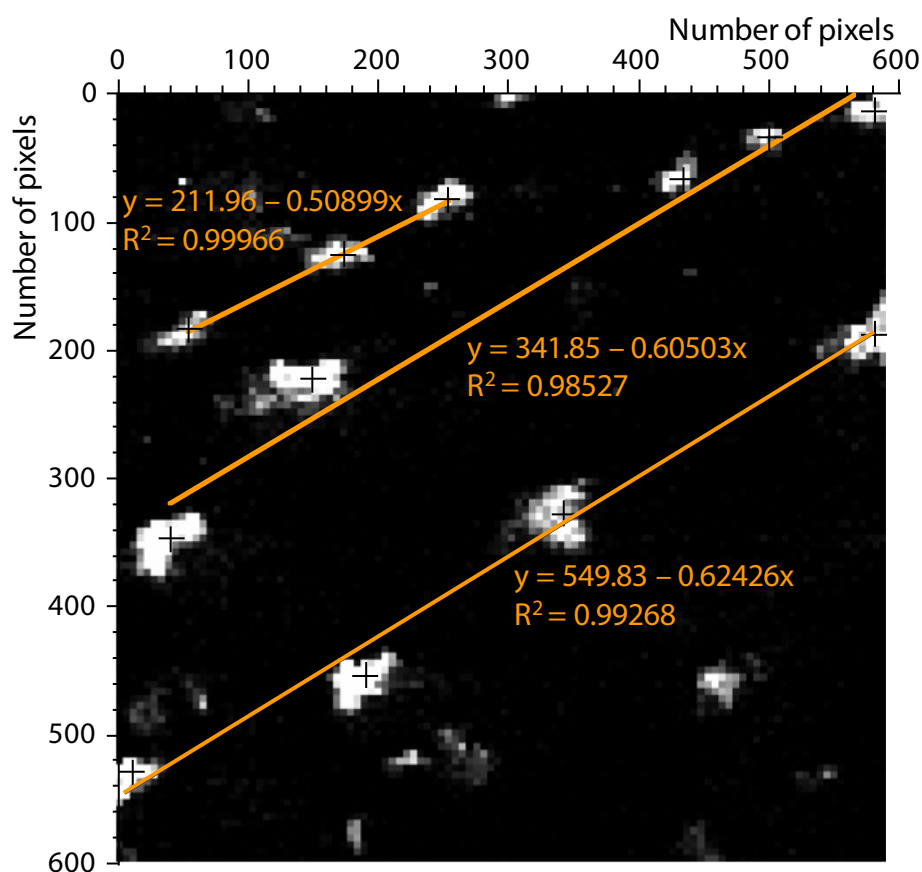
Fig. 7 Analysis of Curcumin Distribution in Axial Section at High Resolution

The center of gravity of the particles was calculated and a linear regression was done through those centers of gravity, showing that the curcumin particles are arranged along a straight line with a high coefficient of determination. The cross marks (+) in the image indicate the positions of the centers of gravity of the particles.
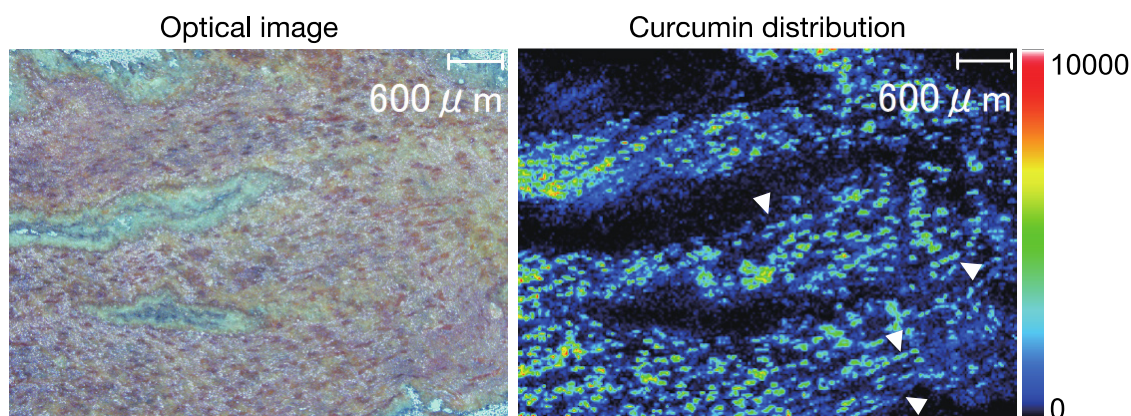

Fig. 8 Curcumin Distribution in Longitudinal Direction

In sections taken near the sample surface in the longitudinal direction, not only the distribution of the particle shape, but also the linear distribution of curcumin can be seen, as shown by the arrowheads.

3-4. Distribution of Curcumin Analogues and Bisacurone in Axial Section

Up to this point, the discussion of this experiment has focused on curcumin ($C_{21}H_{20}O_6$). However, distribution of bisacurone (m/z 251.16) and curcumin analogues with different side chain structures could also be observed, as shown in Fig. 9(A) and Fig. 9(B)-(D), respectively. Fig. 9(E) shows the mass spectrum obtained from a section of turmeric root. All molecules with the exception of bisacurone show similar distributions in the axial section, and the existence of areas where curcumin analogues display a linear distribution was confirmed. This suggests that the curcumin analogues are also enclosed in tube-shaped compartments. On the other hand, this study revealed that the distribution of bisacurone does not show a distinctive accumulation pattern.
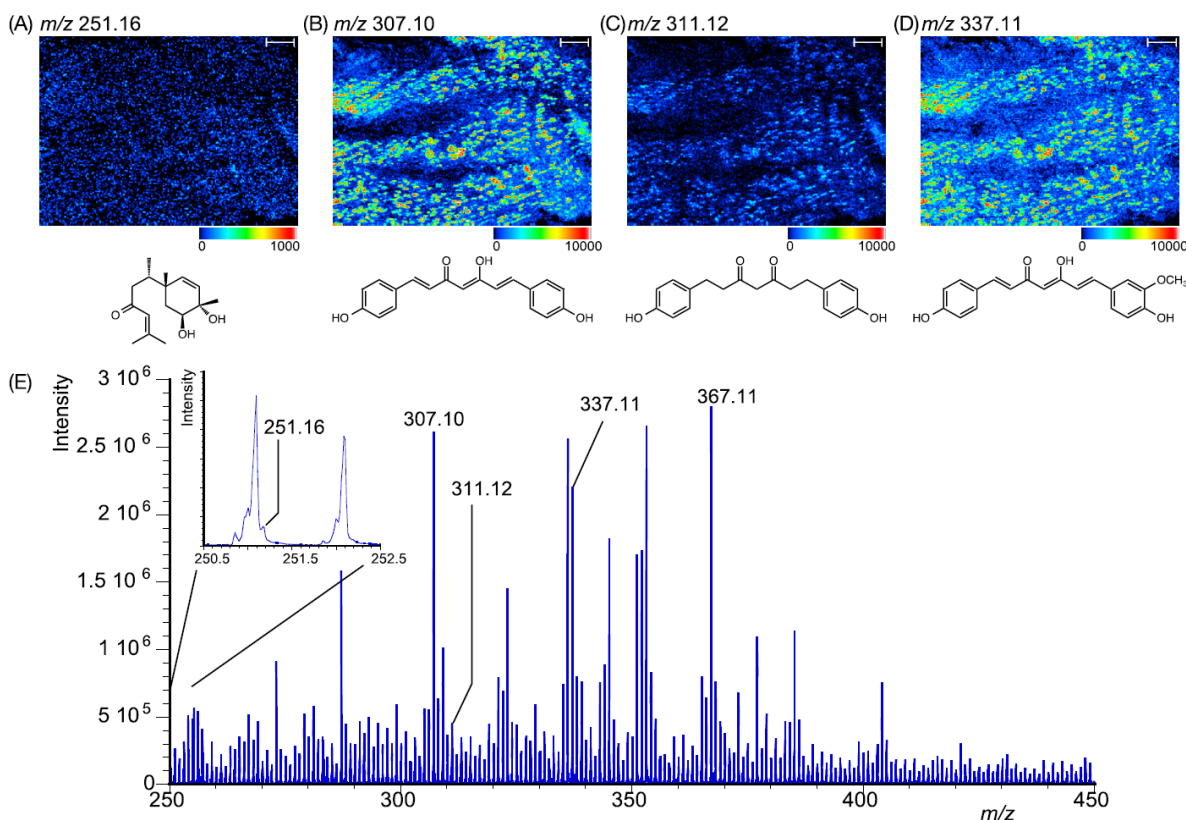
Fig. 9 Distribution Results of Bisacurone and Curcumin Analogues in Axial Section
(A) Distribution of bisacurone,
(B-D) Distributions of curcumin analogues with different side chain structures,
(E) Mass spectrum obtained from section of turmeric root

Because curcumin shows a linear distribution in some areas, it is suggested that tube-shaped compartments exist in the interior of the turmeric, and curcumin is enclosed in those compartments. On the other hand, bisacurone does not display a distinctive distribution, but a uniform distribution.

4. Conclusion

In this research, a dicing machine and a *kanna* (Japanese planer) for sectioning industrial materials were used to prepare samples in order to visualize information on the distribution of curcumin in dried turmeric root. When using the dicing machine, the distribution of curcumin was maintained in the radial section, but the distribution was lost in the axial section. In the section prepared with the *kanna*, the particle shape distribution was also unclear in the radial direction.

For this reason, it is thought that, during sectioning with the dicing machine, friction occurs constantly because the blade of the dicing machine, which rotates at high speed, is in continuous contact with the sample surface, and that the detailed distribution structure is eliminated by this continuous friction. From these results, sectioning using the *kanna* is a more effective method for sample preparation.

In the sections prepared using the *kanna*, the median value of the area of the obtained particle-shaped regions tended to be larger in the axial section than in the radial section, as shown in Fig. 5(D), suggesting that the particles are not perfectly spherical. This is similar to the results for 6-gingerol shown in Fig. 3. The observed distributions show that not only the particle size, but also the particle shape is different. When this difference in shape was evaluated by oblateness, it was found that the oblateness was 0.42 of the particles in the axial section. Although a biphasic distribution could be seen in the radial section, the peak of oblateness was near 0.3. In other words, the particles display a nearly-round shape in the radial section but an approximately elliptical shape in the axial section.

Furthermore, the 5 μm imaging results in Fig. 6 show extremely regular distributions in both the axial section and the radial section. Specifically, regular ellipses aligned in the axial section, and a particle distribution density was high in the central part of the turmeric in the radial section. This result supports the conclusion that the distribution of curcumin in turmeric has a distinctive structure. In particular, from the results of the image analysis shown in Fig. 7, it can be concluded that a regular particle alignment exists in the axial section. One extremely interesting point obtained from the fitting results is the constant slope of all the lines of best fit through the particles. The existence of elliptical particles in the axial section, as shown in Fig. 5, and their alignment in a straight line, as shown in Fig. 6, suggested that the central part of turmeric has a tubular structure. Fig. 8 shows a large number of areas showing a linear distribution in the axial section image, which seems to support this tubular structure. Moreover, while the analogues of curcumin also displayed a similar distribution, no distinctive distribution of bisacurone could be observed. Thus, considering the imaging results of the radial section and axial section, it is suggested that a tubular structure containing curcumin exists in the turmeric root.

In this research, a technique for visualizing the distribution of curcumin was developed using a dried turmeric root, and a detailed analysis of the distribution of curcumin was conducted. Axial sections and radial sections for mass spectrometry imaging (MSI) could be prepared by using the *kanna*, and the results suggest that the interior of the turmeric root has an extremely regular structure, specifically, a tubular structure in which curcumin is enclosed. This research is the first example of application of MSI to a hard dried material, and suggests the possibility of visualizing the distributions of secondary metabolites in various other sample materials. By obtaining information on the spatial distribution of active ingredients in this manner, it will be possible to obtain ground products with high contents of the targeted active ingredient. This information will be useful not only for direct use of ground products as raw materials, but also in pretreatment processes for extracting specific active ingredients.

<References>
(1) Taira, S et al.   *J. Agric. Food Chem.* **2015**, *63* (27), 6109-12.
(2) Shroff, R et al.   *Proc. Natl. Acad. Sci. U. S. A.* **2008**, *105* (16), 6196-201.
(3) Grassl, J. et al.   *Plant Methods* **2011**, *7* (1), 21.
(4) Mullen, A. K et al.   *Rapid Commun. Mass Spectrom.* **2005**, *19* (18), 2507-16.
(5) Ohtsu, S et al.   *Analytical Sciences* **2018**, *34* (9), 991-996.
(6) Niehoff, A. C et al.   *Anal. Chem.* **2014**, *86* (22), 11086-92.
(7) Urban, P. L et al.   *Anal. Chem.* **2011**, *83* (10), 3918-25.
(8) Nguyen, T. B et al.   *Appl. Environ. Microbiol.* **2018**, *84* (9).
(9) Dunham, S. J. B et al.   *Acc. Chem. Res.* **2017**, *50* (1), 96-104.
(10) Kompauer, M et al.   *Nat. Methods* **2017**, *14* (1), 90-96.
(11) Moree, W. J et al.   *Proceedings of the National Academy of Sciences* **2012**, *109* (34), 13811-13816.
(12) Phelan, V. V et al.   *J. Am. Soc. Mass Spectrom.* **2015**, *26* (6), 873-7.
(13) Yang, Y. L et al.   *Nat. Chem. Biol.* **2009**, *5* (12), 885-7.
(14) Taira, S et al.   *Am. J. Chin. Med.* **2010**, *38* (3), 485-93.
(15) Miyoshi, K et al.   *Analytical Sciences* **2018**, *34* (9), 997-1001.
(16) Franceschi, P et al.   *J. Exp. Bot.* **2012**, *63* (3), 1123-33.
(17) Crecelius, A. C et al.   *J. Agric. Food Chem.* **2017**, *65* (17), 3559-3568.
(18) Dalisay, D. S et al.   *J. Nat. Prod.* **2015**, *78* (6), 1231-42.
(19) Holscher, D et al.   *Plant J.* **2009**, *60* (5), 907-18.
(20) Soares, M. S et al.   *Phytochemistry* **2015**, *115*, 161-170.
(21) Taira, S et al.   *International Journal of Biotechnology for Wellness Industries* **2012**, *1* (1), 61-65.
(22) Shimma, S et al.   *J. Agric. Food Chem.* **2019**, *67* (34), 9652-9657.
(23) Harada, T et al.   *Anal. Chem.* **2009**, *81* (21), 9153-9157.
(24) Nakamura, J et al.   *Anal. Bioanal. Chem.* **2017**, *409* (6), 1697-1706.
(25) Yang, J et al.   *Anal. Chem.* **2011**, *83* (14), 5728-34.

SHIMADZU

Shimadzu Corporation

www.shimadzu.com/an/